

Available online at www.sciencedirect.com**ScienceDirect**

Procedia CIRP 13 (2014) 84 – 89

www.elsevier.com/locate/procedia2nd CIRP 2nd CIRP Conference on Surface Integrity (CSI)

Comparison of surface textures generated in hard turning and grinding operations

Wit Grzesik^a, Krzysztof Żak^{a*}, Piotr Kiszka^a^a*Opole University of Technology, Str. Mikolajczyka 5, 45-271 Opole Poland** Corresponding author. Tel.: +48-774498462; fax: +48-774499927. E-mail address: k.zak@po.opole.pl.

Abstract

The problem of replacing costly and environmentally detrimental grinding operations by hard turning or milling processes needs further investigations related to the obtainable quality of machined parts. In author's opinion the problem should be extended to the surface texture generated in these contrary operations which is critical for service properties demanded by end-users. Taking these aspects into consideration, an extended study was performed to characterize surface topographies (3D surface roughness parameters) produced. In this case study, the turned and ground surfaces with the same Ra roughness parameter of about 0.3 μm were compared. Moreover, the frequency, furrows, fractal and motifs analyses have aided the final conclusions. The analysis done would assist technologists to select an optimum chain of machining operations.

© 2014 The Authors. Published by Elsevier B.V. Open access under [CC BY-NC-ND license](https://creativecommons.org/licenses/by-nc-nd/4.0/).Selection and peer-review under responsibility of The International Scientific Committee of the "2nd Conference on Surface Integrity" in the person of the Conference Chair Prof Dragos Axinte dragos.axinte@nottingham.ac.uk*Keywords:* surface texture; hard machining; grinding

1. Introduction

Machining of hardened steels (45-60 HRC) with ultrahard cutting tool materials has been an alternative for grinding for three decades and now is increasingly used in large-batch and mass production for high performance components [1,2]. High flexibility, possible complete machining, less ecological impact and higher MRR are the main advantages of hard machining over grinding [3-4]. On the other hand, its industrial use is still limited due to some negative effects on surface integrity and the attainable accuracies [3,5]. Special attention is paid to precision and high-precision hard turning operations for which the achievable Rz roughness parameter is set at 2.5-4 μm and below 1 μm respectively [2]. The discussion platform-hard cutting vs. grinding is extended to the capability profiles of both these operations to the functionality of the machined surfaces [6]. In this aspect a special focus should be made on surface finish and surface texture induced by these challenged operations [7,8]. This is because hard turning and grinding generate different surface structures

which influence their functional properties, predominantly the fatigue strength. As a result, their comparison in terms of the geometrical quality needs both 2D and 3D surface roughness parameters to be determined. First such attempt which includes 2D height and amplitude parameters and the BACs is presented in Ref. [6]. These analyses showed the dissimilarity between the hard turned and ground surface topographies although the Ra or Rz parameters are nearly the same. This evidence was confirmed in Ref. [7] when comparing 3D surface topographies produced by CBN hard turning and grinding using an Al_2O_3 wheel. In this comparison AISI 52100 steel of 61-62 HRC was machined. The 2D and 3D comparison, more oriented on bearing area parameters, related to precision hard turning and belt grinding is provided in Ref. [8]. The objective of this study is to comprehensively characterize and compare surface textures of representative hard turned and ground surfaces using a number of standardized 3D roughness parameters as well as other characteristics such as fractal dimensions, motifs and frequency parameters. The comparative

criterion assumes that in both cases the Ra(Sa) parameter is about 0.3 μm .

2. Experimental procedure

2.1. Machining conditions

This experimental study includes finish hard turning and grinding operations on specimens made of a 41Cr4 (AISI 5140 equivalent) steel with Rockwell's hardness of 57 ± 1 HRC and initial Sa roughness of about 0.4 μm . Workpieces were turned with constant cutting parameters which permit the Ra roughness of about 0.2 μm using low content CBN tools containing about 60% CBN, grade CB7015 by SandvikCoromant. TNGA 160408 S01030 chamfered inserts with brazed-CBN tips were used. The machine tool was a CNC turning center, Okuma Genos L200E-M. Grinding operations were performed on a conventional cylindrical grinder using monocrystalline aloxite Al_2O_3 wheel and water soluble emulsion as a coolant. Machining conditions for cutting and abrasive operations are specified in Table 1.

Table 1. Hard turning and cylindrical grinding conditions

Symbol	Machining operation	Machining conditions
INIT-HT	Hard turning using CBN TNGA 160408 S01030 chamfered insert	$v_c=150$ m/min, $f=0.1$ mm/rev, $a_p=0.15$ mm
HT		$v_c=150$ m/min, $f=0.075$ mm/rev $a_p=0.15$ mm
GR	Cylindrical multi-stage grinding using Al_2O_3 ceramic wheel, 350 \times 25 \times 127 32A	$v_c=11.9$ m/s $a_c=0.025$ mm $f_a=3.5$ m/min 5 passes plus spark-out

2.2. Characterization of surface topography

Surface topographies generated by HT and GR operations were recorded using a TOPO-01P contact profilometer with a diamond stylus radius of 2 ± 0.5 μm . The determination of 3D roughness parameters and 3D visualization of machined surfaces were performed using a Digital Surf, Mountains® Map package. The characterization of surface topographies was based on three groups of parameters including:

- standardized five subgroups of 3D surface roughness parameters: height, amplitude, horizontal, hybrid and functional [9],
- fractal dimensions determined by the method of enclosing boxes,
- standardized motifs parameters, and
- characteristics of frequency spectra recorded.

3. Experimental results and discussion

This part highlights the obtained results and their importance in permitting high quality and functional properties required for highly and dynamically loaded parts finished by precision hard turning and gentle grinding operations.

3.1. Characterization of surface topography

Representative surface profiles and topographies obtained in hard turning and grinding operations performed are presented in Figs. 1 and 2 respectively. From the practical point of view, of fundamental importance is the comparison of the arithmetic mean height Sa (Ra) and maximum surface height Sz (Rz) which are frequently used by constructors and technologists. In terms of the surface quality criterion discussed in the Introduction both operations can be classified as precision machining, although hard turning is close to high-precision machining for which Rz parameter should be less than 1 μm (the measured Rz is equal to 1.2 μm).

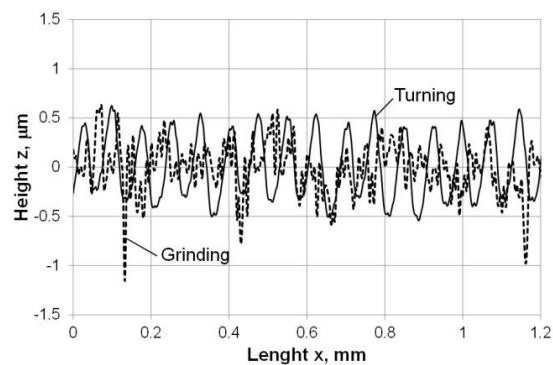


Fig. 1. Overlay of the surface profiles generated by HT and grinding

The measured values of Sa and Sz parameters are equal to 0.28 μm and 1.6 μm for hard turning, and 0.27 μm and 4 μm for grinding. It should be noted that 2D values of Rz are substantially lower and equal to 1.2 and 2.4 μm for hard turned and ground surfaces respectively. This comparison clearly depicts that ground surfaces contain a number of high sharp peaks which increase distinctly the maximum surface height Sz, in this case study up to 4 μm , although the Sa parameter is equal to about 0.3 μm . Hence, the comparison of these surface textures keeping constant Rz parameter given in Ref. [6] seems to be questionable. This observation is further confirmed by visualization of both surface profile and surface topography generated by CBN cutting tool and aloxite ceramic wheel presented successively in Figs. 1 and 2. Fig. 1 presents superimposed surface profiles with the same value of Ra (Sa) parameter produced by hard

turning and grinding operations. As shown in Fig. 1, the grinding of the hard turned surface causes that regular (deterministic) surface profile generated by hard turning with a small feed rate becomes partly random with deep notches which negatively influence fatigue strength.

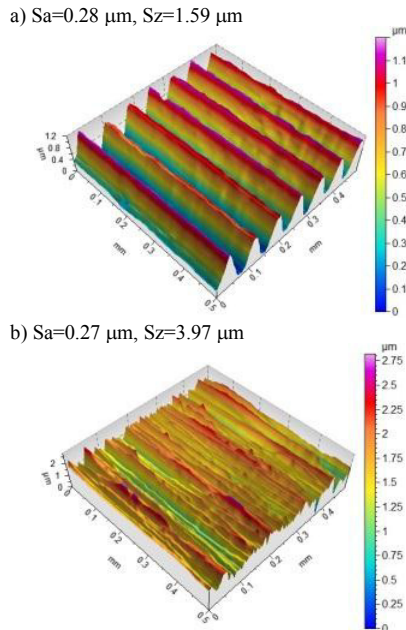


Fig. 2. Surface textures produced by HT (a) and grinding (b); zoomed isometric views

The regular distribution of feed-marks characteristic for CBN turned surface with small feed rate is visualized in Fig. 2a. In this case a special zooming technique of the surface isometric view was used. The ground surface shown in Fig. 2b contains periodic components and the distances between them agree roughly with the wave lengths presented in the PSD spectrum shown in Fig. 7a.

3.2. Characterization of area bearing properties

Fig. 3 presents the shapes of 3D BAC and associated ADF curves obtained for the compared machining operations. In particular, hard turning produces surfaces with near linear BAC (1) with distinctly higher material ratio $S_{mr}(20)$ and finish grinding generates surfaces with S-shape BAC (2) and negative skewness S_{sk} . It is worth noticing that the values of skewness R_{sk} and S_{sk} for ground surfaces differ visibly- (-0.60) versus (-0.20). Similar values of S_{sk} parameter for HT and GR operations (positive and negative) are reported in Ref. [7]. On the other hand for anisotropic-periodic turned surfaces with regular ridges they are equal $R_{sk}=S_{sk}=0.13$. Moreover, Fig. 3b suggests that hard turning and grinding produced topographies with diametrically different ADF shapes.

In addition, three functional parameters associated with the 3D BAC, namely the surface bearing index (S_{bi}), the core fluid retention index (S_{ci}) and the valley fluid retention index (S_{vi}) [9-11], which characterize bearing and oil retention properties were taken into account.

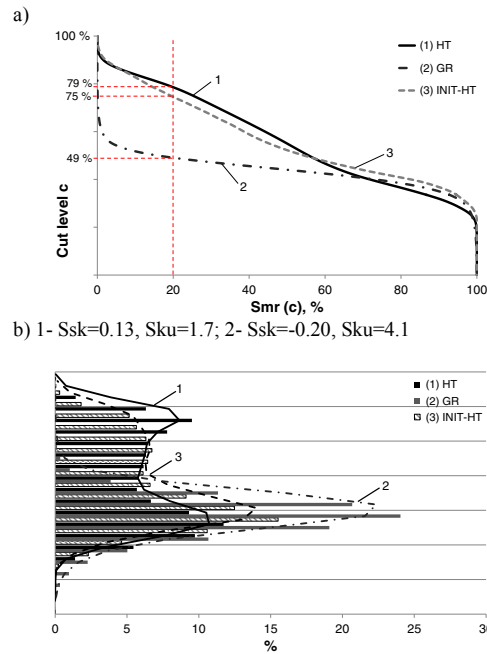
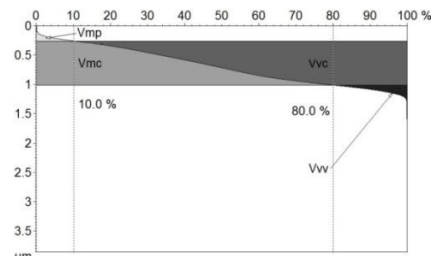


Fig. 3. 3D BAC (a) and ADF (b) for HT and grinding

a) ($V_{mp}=0.00533 \text{ ml/m}^2$, $V_{vc}=0.424 \text{ ml/m}^2$, $V_{mc}=0.329 \text{ ml/m}^2$, $V_{vv}=0.0171 \text{ ml/m}^2$)



b) ($V_{mp}=0.0173 \text{ ml/m}^2$, $V_{vc}=0.386 \text{ ml/m}^2$, $V_{mc}=0.298 \text{ ml/m}^2$, $V_{vv}=0.0475 \text{ ml/m}^2$)

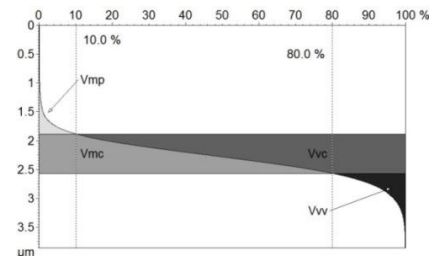


Fig. 4. Volume functional parameters for turned (a) and ground (b) surfaces

Smaller value of surface bearing index $S_{bi}=0.20$ for ground surface indicates lower wear of peaks (for the Gaussian surface, $S_{bi}\approx 0.61$). On the other hand, the values of core fluid retention index $S_{ci}=1.48$ (HT) and 1.40 (GR) suggest compared fluid retention of both the turned and ground surfaces (for the Gaussian surface, the $S_{ci}\approx 1.56$). Moreover, larger value of valley fluid retention index $S_{vi}=0.07$ for the ground surface ($S_{vi}=0.05$ for turned surface) indicates better fluid retention ability in the valley zone. (for the Gaussian surface, the $S_{vi}\approx 0.11$).

The functional analyses of the 3D BAC can be extended to the next three volume parameters including the material volume of the surface (V_m), the core void volume (V_{vc}) and the valley void volume (V_{vv}) parameters.

At first glance, these parameters represent volumes equivalent to the S_{bi} , S_{ci} and S_{vi} indices and their interpretations have the same meanings [9]. Their distributions and values obtained for HT and GR operations are presented in Fig. 4.

For instance, higher value of valley void volume $V_{vv}=0.0475$ ml/m² confirms, in addition to higher values of valley fluid retention index S_{vi} , better fluid retention ability of ground surfaces.

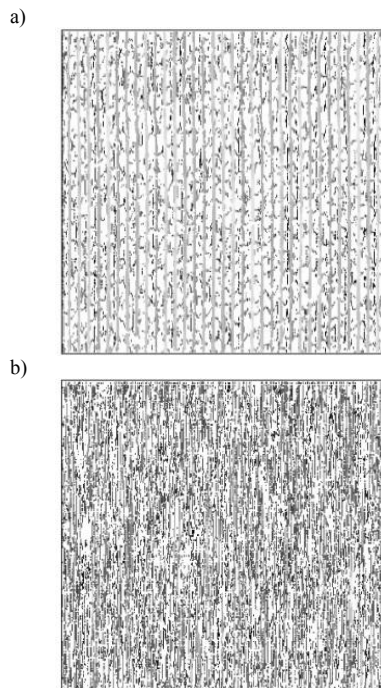


Fig. 5. Vectorized micro-valleys networks for turned (a) and ground (b) surfaces

Additional information on the fluid retention between the matted surfaces can be obtained using an original technique of the vectorisation of micro-valleys network

generated on the machined surface [10,11]. Characteristic nets of micro-grooves visualized for turned and ground surfaces are illustrated in Fig. 5. The maximum depth of valleys is equal to $1.1\ \mu\text{m}$ and $2.1\ \mu\text{m}$ and their widths are equal to 0.5 and $0.6\ \mu\text{m}$. Additionally, the average density of valleys is equal to 422 and 665 cm/cm² respectively. These data coincides well with the distributions of the volume functional parameter (V_{vv}) shown in Fig. 4. Moreover, vectorial images shown in Fig. 5 confirm that the generated surfaces are periodic anisotropic (Fig. 5a) and mixed periodic-random anisotropic (Fig. 5b).

3.3. Area spatial and hybrid parameters

The set of 3D parameters includes four spatial parameters among which three are texture parameters. The ground surfaces contain distinctly more summits within the scanned area- $S_{ds}=1305.6$ 1/mm² versus 1123.9 1/mm² for turned surfaces. The smaller texture aspect ratio $Str=0.01$ for turned surfaces indicates stronger directionality (anisotropy) but its values for both operations which are less than 0.1 are characteristic for highly anisotropic surfaces [9]. The texture direction Std close to 90° indicates that the dominant surface lay is perpendicular to the measurement direction. The values of Sal parameter (the fastest decay autocorrelation length) obtained (0.02 mm vs. 0.01 mm) suggest that the turned texture is dominated to a greater extent by long wavelength feed-marks whereas the ground texture is dominated by short wavelength patterns. This conclusion agrees with the APS spectra shown in Fig. 7.

The values of three 3D hybrid parameters emphasize additional geometrical differences in the textures of both compared surfaces. The ground surfaces contain irregularities with higher slopes S_{dq} -about 70 versus 30 for turned surfaces. This trend coincides qualitatively with 2D slope data. The value of the average summit curvature S_{sc} of about $0.007\ \mu\text{m}^{-1}$ for the turned surface and $0.018\ \mu\text{m}^{-1}$ for the ground surface agrees with those for typical machined surfaces (0.004 - $0.03\ \mu\text{m}^{-1}$) given in [9]. The developed interfacial area ratio S_{dr} is higher for ground surfaces for which the smallest unit of plane area is about $0.24\ \%$. On the other hand, the regular turned surface (Figs. 2a1 and 2a2) contains less irregularities and, in turn, S_{dr} is smaller (0.04%) than for the ground surface.

3.4. Motifs and fractals

The motif analysis is performed on the unfiltered surface profile divided into a series of windows [11,12], as shown in Fig. 6. The three parameters-the mean depth

of roughness motif R, the mean spacing of roughness motif AR and the largest motif height Rx were analysed.

The comparison of motif parameters indicates that ground surfaces include distinctly deeper pits ($R_x=2.55 \mu\text{m}$) than hard-turned surfaces ($R_x=1.25 \mu\text{m}$) which is in accordance with the overlapped surface profiles shown in Fig. 1 and volume bearing parameters shown in Fig. 4. In addition, for the hard-turned surface the value of $AR=0.08 \text{ mm}$ is equal to the feed rates applied ($f=0.075 \text{ mm/rev}$) and mean line peak spacing $R_{sm}=0.07 \text{ mm}$. The distribution of motif windows for the ground surface confirms enhanced fluid retention in comparison to the turned surface with a comparable arithmetic mean height S_a value.

The values of fractal dimension S_{fd} determined by means of the method of enclosing boxes are equal to 2.31 and 2.39 for turned and ground surfaces respectively. It should be noted that the higher value of fractal dimension depicts the presence of randomly distributed fragments of the machined surface (its value equals 3 means full chaotic and random surface structure).

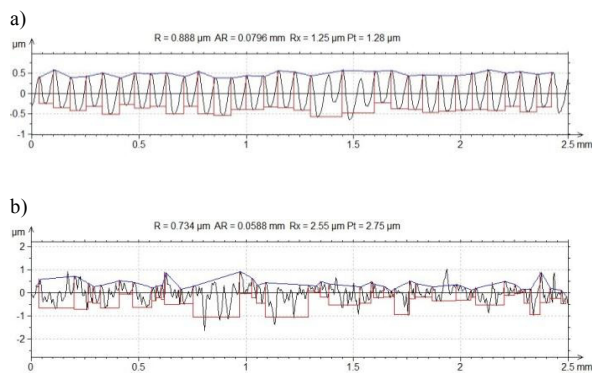


Fig. 6. Motif graphs for HT (a) and grinding (b)

3.5. Frequency analysis

The PSD spectra obtained for hard turned and ground surfaces are presented in Fig. 7. This parameter is very sensitive for all disturbances of the generated surfaces which appear in the technological machining system. It is evident in Fig. 7a that in hard turning machining surface is generated without cutting vibrations and the PSD spectrum contains only one low-frequency component with the wave length the same as the feed rate of 0.075 mm ($75 \mu\text{m}$) and the amplitude of $0.26 \mu\text{m}$. On the other hand, the ground surface (Fig. 7b) is generated with the presence of machining vibrations and the PSD spectrum contains, despite the basic component of $108 \mu\text{m}$ in length, some additional components resulting from periodic disturbances (of $135 \mu\text{m}$ and $202 \mu\text{m}$ in length in Fig. 7b).

The structures of generated surfaces can be easily recognized by means of the images of the appropriate autocorrelation functions (AACF) presented in Fig. 8.

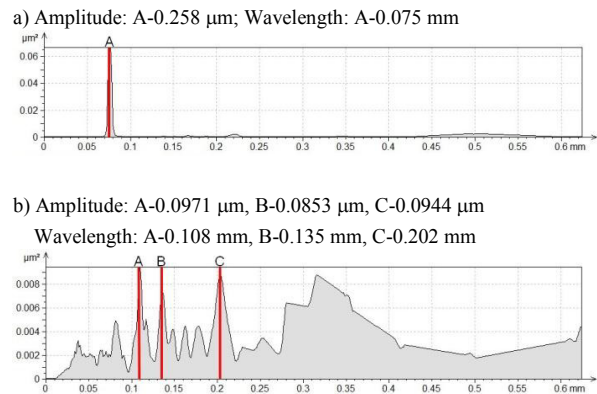


Fig. 7. Averaged power spectral density for turned (a) and ground (b) surfaces

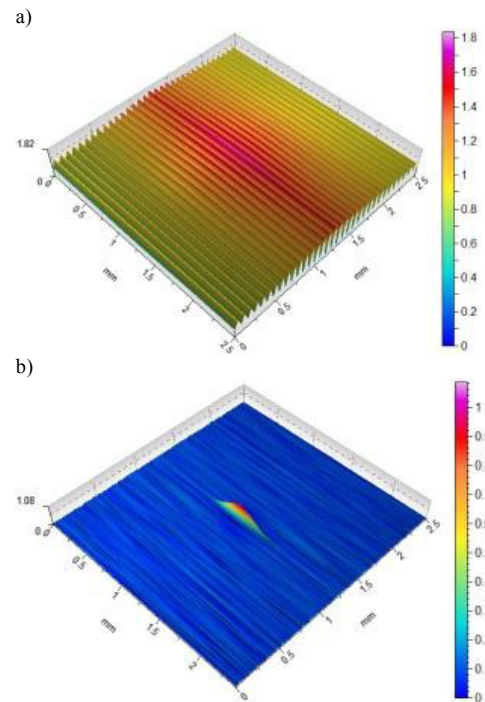


Fig. 8. Representative autocorrelation functions for turned (a) and ground (b)

From this point of view, the turned surface is periodic-anisotropic (Fig. 8a) but the ground surface is mixed, between anisotropic and random structures. In the second case (Fig. 8b) also an exponential function with characteristic decay of the periodicity is depicted. Moreover, the content of isotropy in the ground surfaces is about 3.5% (for turned surface is less than 1%).

Conclusions

1. Although attributes of turned and ground surfaces are described by the same average roughness Ra of about 0.3 μm their spatial features are different. This fact suggests that their functional properties should also be different.
2. The textures of hard turned and ground surfaces are periodic-anisotropic and mixed periodic-random anisotropic respectively. This difference can be determined based on 3D surface topographies, the distributions of the PSD (APSD) function as well as vectorial maps of micro-valleys. However, the disturbances of regular surface structures by grinding can result from both the kinematical and tribological effects.
3. 3D BAC curves and appropriate functional parameters depict that ground hard surfaces have better bearing properties. This is due to negative skewness Ssk value and lower surface bearing index Sbi value for ground topographies.
4. It was documented, based on vectorial maps of micro-valleys that ground surfaces indicate better fluid retention ability. This is due to deeper and wider grooves as well as higher average density of valleys.
5. Distinct differences between 2D and 3D roughness parameters were revealed for periodic-random surfaces represented in this case study by ground surfaces. As a result, the replacing of ground surfaces by hard turned surfaces based on 2D roughness data can be highly risky.

- [11] de Chiffre, L., Lonardo, P.M., Trumpold, H., et al., 2000. Quantitative characterization of surface texture, CIRP Annals-Manufacturing Technology 49, p. 635.
- [12] Lou, S., Jiang, X., Scott, P.J., 2013. Correlating motif analysis and morphological filters for surface texture analysis, Measurement 46, p. 993.

References

- [1] Tönshoff, H.K., Arendt, C., Ben Amor, C., 2000. Cutting of hardened steel, CIRP Annals-Manufacturing Technology 49, p. 547.
- [2] Klocke, F., 2011. Manufacturing processes 1. Cutting, Springer, Berlin.
- [3] Köning, W., Bertold, A., Koch, K.F., 1993. Turning versus grinding—a comparison of surface integrity aspects and attainable accuracies. CIRP Annals 42/1, p. 39.
- [4] Davim, J.P., Editor, 2011. Machining of hard materials, Springer, London.
- [5] Bartarya, G., Choudhury, S.K., 2012. State of the art in hard turning, International Journal of Machine Tools and Manufacture 53, p. 1.
- [6] Klocke, F., Brinksmeier, E., Weinert, K., 2005. Capability profile of hard cutting and grinding processes, CIRP Annals-Manufacturing Technology 54, p. 557.
- [7] Waikar, R.A., Guo Y.B., 2008. A comprehensive characterization of 3D surface topography induced by hard turning versus grinding, Journal of Materials Processing Technology 197, p. 189.
- [8] Grzesik, W., Rech, J., Wanat, T., 2007. Surface finish on hardened bearing steel parts produced by superhard and abrasive tools, International Journal of Machine Tools and Manufacture 47, p. 255.
- [9] Griffiths, B., 2001. Manufacturing surface technology. Surface integrity and functional performance, Penton Press, London.
- [10] Lonardo, P.M., Trumpold, H., de Chiffre, L., 1996. Progress in 3D surface microtopography characterization, CIRP Annals-Manufacturing Technology 45, p. 589.